Molecular mechanisms underlying nucleocytoplasmic shuttling of actinin-4

Masahiro Kumeta[1,*], Shige H. Yoshimura[1], Masahiko Harata[2] and Kunio Takeyasu[1]

[1]Graduate School of Biostudies, Kyoto University, Kyoto 606-8501, Japan
[2]Graduate School of Agricultural Science, Tohoku University, Sendai 981-8555, Japan
*Author for correspondence (kumeta@lif.kyoto-u.ac.jp)

Accepted 19 December 2009
Journal of Cell Science 123, 1020-1030

doi:10.1242/jcs.059568

Summary

In addition to its well-known role as a crosslinker of actin filaments at focal-adhesion sites, actinin-4 is known to be localized to the nucleus. In this study, we reveal the molecular mechanism underlying nuclear localization of actinin-4 and its novel interactions with transcriptional regulators. We found that actinin-4 is imported into the nucleus through the nuclear pore complex in an importin-independent manner and is exported by the chromosome region maintenance-1 (CRM1)-dependent pathway. Nuclear actinin-4 levels were significantly increased in the late G2 phase of the cell cycle and were decreased in the G1 phase, suggesting that active release from the actin cytoskeleton was responsible for increased nuclear actinin-4 in late G2. Nuclear actinin-4 was found to interact with the INO80 chromatin-remodeling complex. It also directs the expression of a subset of cell-cycle-related genes and interacts with the upstream-binding factor (UBF)-dependent rRNA transcriptional machinery in the M phase. These findings provide molecular mechanisms for both nucleocytoplasmic shuttling of proteins that do not contain a nuclear-localization signal and cell-cycle-dependent gene regulation that reflects morphological changes in the cytoskeleton.

Key words: INO80 complex, NOR, Actinin, Cell cycle, Nucleocytoplasmic shuttling

Introduction

α-Actinin is a well-known crosslinking protein that bundles actin filaments at focal-adhesion sites. Evolutionary analysis suggests that this protein best resembles the ancestral proteins of the spectrin superfamily, which is characterized by ubiquitously conserved spectrin repeats (SRs) and found in a large variety of taxa (Virel and Backman, 2004). In addition to its structural role as a crosslinker of actin filaments, α-actinin is known to serve as a platform for a number of protein-protein interactions within the cytoskeletal organization (reviewed in Otey and Carpen, 2004; Sjoblom et al., 2008).

α-Actinin-4 (hereafter referred to as actinin-4) was first described in 1998 as a novel isoform of non-muscle α-actinin (Honda et al., 1998). Four isoforms of α-actinin are expressed in a tissue-specific manner in humans. Actinin-2 and -3 are specifically expressed in muscle cells, whereas actinin-1 and -4 are ubiquitously expressed (Beggs et al., 1992; Millake et al., 1989; Youssoufian et al., 1990). The actinin molecule is divided into three functional subdomains: an N-terminal actin-binding domain, which is composed of two calponin homology domains (CH1 and CH2); the C-terminal EF-hands; and the central rod domain, which is composed of four spectrin repeats (SR1-SR4) (Davison and Critchley, 1988; Mimura and Asano, 1987). Antiparallel dimerization of the molecule results in the formation of a dimer with an actin-binding domain located at both ends. Dimer formation is required for its normal function as a crosslinker of the actin cytoskeleton (Ylanne et al., 2001). In addition to its homodimeric interaction, the α-actinin isoforms are also known to associate with numerous other factors involved in focal-adhesion formation. Triple-helical SR4 in α-actinin directly binds to the adhesion-complex protein vinculin (Bois et al., 2005). Microinjection of the vinculin-binding site (VBS) of α-actinin into 3T3 cells has been shown to inhibit the normal α-actinin–vinculin interaction and induces cytoskeletal collapse (Bois et al., 2006), suggesting that this molecular interaction plays a key role in the maintenance of focal adhesions.

Although the α-actinin isoforms are approximately 84% identical and share 90% similarity in their amino acid sequences, the two non-muscle isoforms of α-actinin, actinin-1 and -4, exhibit vastly different behaviors in vitro and in vivo. By contrast to the high sensitivity of actinin-1 to calcium concentration, actinin-4 is different in that its C-terminal EF-hands confer lower calcium sensitivity (Imamura et al., 1994; Nikolopoulos et al., 2000). Fluorescence ratio imaging analysis of highly motile cells, such as macrophages, has revealed that actinin-4 is more concentrated in the circular ruffles located on the dorsal surface, whereas actinin-1 is evenly distributed in all F-actin structures, such as the dorsal and peripheral edge ruffles, phagocytic cups and basal podosomes (Araki et al., 2000). These findings suggest that these two isoforms play an important role in distinct cytoskeletal functions and thus might be regulated in a different manner.

Actinin-4 has also been shown to localize to the nucleus. Upon inhibition of phosphoinositide 3-kinase (PI3 kinase) or actin depolymerization, significant nuclear accumulation of actinin-4 was observed in several cancer cell lines (Honda et al., 1998). This nuclear accumulation was also observed in A431 cells treated with tumor necrosis factor (TNF) or epidermal growth factor (EGF) in association with the p65 subunit of nuclear factor (NF)-κB. These findings most probably indicate a specific role for actinin-4, as actinin-1 has not been detected in the nucleus to date (Babakov et al., 2008). Several proteins that play an important structural role in the cytoplasm are also localized to the nucleus, including SR-containing proteins such as the spectrins, nesprins, bullous pemphigoid antigen 1 (Bpag1) and nuclear mitotic apparatus protein (NuMA) (Young and Kothary, 2005). These proteins must

be controlled by an as-yet-unidentified nuclear-localization mechanism, as their large molecular size (greater than 70 kDa) renders them unable to diffuse through the nuclear pore complex (NPC). Although Bpag1 contains a conserved nuclear localization signal (NLS) within the SR domain (Young et al., 2003), the other SR-containing proteins lack an obvious NLS. It is not clear how these large non-NLS proteins become localized to the nucleus. Given its large molecular mass (105 kDa) and its apparent lack of NLS, the precise molecular mechanisms underlying nuclear transport of actinin-4 remain largely unknown.

In this study, we investigate the molecular mechanisms underlying nucleocytoplasmic shuttling of actinin-4 and reveal that the nuclear localization of actinin-4 alters during cell-cycle progression. We also identified a novel function for actinin-4 in cell-cycle-dependent transcriptional regulation in relation to the INO80 chromatin-remodeling complex and the mitotic-specific association of actinin-4 with the rRNA transcriptional machinery, suggesting multiple roles for this molecule in cell-cycle-dependent nuclear events.

Results

Subcellular localization of actinin-4

We generated a specific monoclonal antibody, #92B, from a set of antibodies raised against nuclear structural proteins in HeLa cells (web database: http://www.lif.kyoto-u.ac.jp/labs/chrom/abgallery/index.html). The epitope of this antibody was one of the triple helices of SR4 (amino acid residues 735-759) (Fig. 1A), which is known to serve as a VBS that swings out from the molecule to expose its hydrophobic face (Bois et al., 2005). We did not observe any obvious cross-reactivity between antibody #92B and other proteins using western blot analysis (Fig. 1B). The intensity of the protein band recognized by #92B and anti-actinin-4 polyclonal antibody decreased to a similar level when the cells were subjected to siRNA-directed knockdown of actinin-4 (Fig. 1C). By contrast, the amount of actinin-1 and α-tubulin remained unaffected. These results demonstrated that #92B reacts specifically with actinin-4.

The subcellular localization of actinin-4, detected by #92B, suggested that actinin-4 is present in several molecular forms. Anti-actinin-4 polyclonal antibody predominantly stained the focal

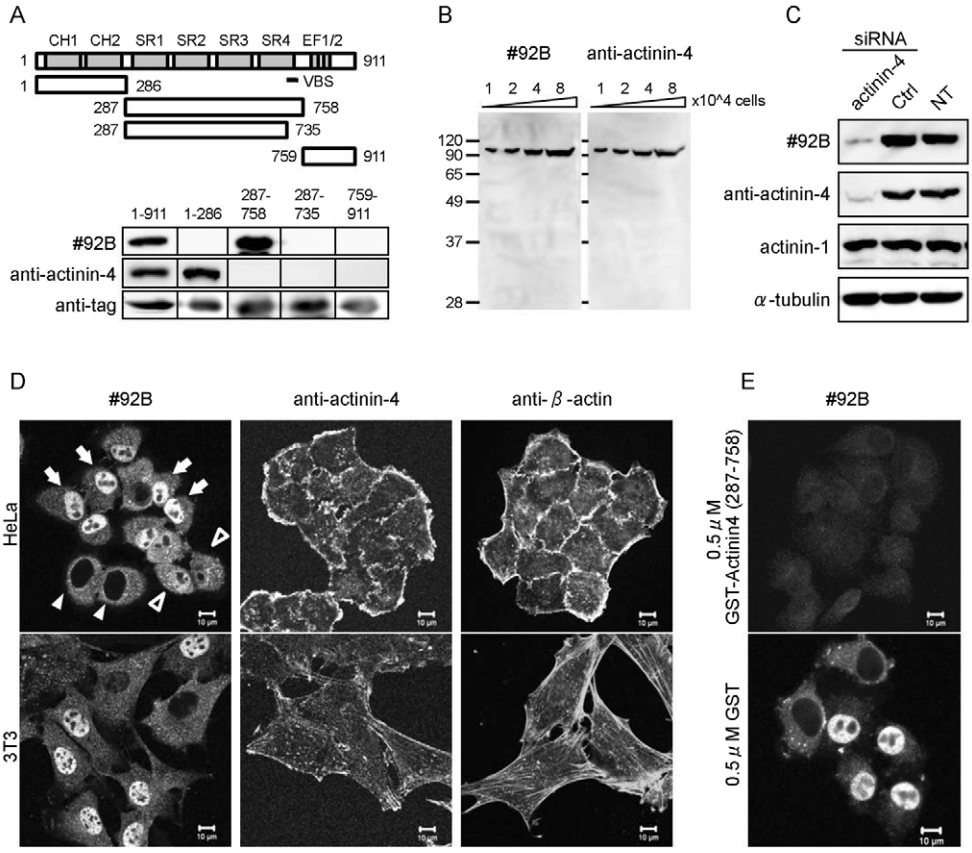

Fig. 1. Monoclonal antibody #92B recognizes vinculin-free forms of nuclear actinin-4. (**A**) Epitope mapping analysis by western blot. His-tagged full-length actinin-4 and GST-tagged fragments corresponding to the actin-binding domain (amino acid residues 1-286), central SR region (287-758), SR region ΔVBS (287-735) and C-terminal EF-hand region (759-911) were constructed and expressed in bacteria. Western blot analysis of each fragment was performed using #92B, anti-actinin-4 polyclonal antibody, and anti-His and anti-GST antibodies. (**B**) Western blot analysis of HeLa whole-cell lysate using #92B. The cells were lysed in 5% SDS buffer and subjected to SDS-PAGE following #92B immunoblot detection. (**C**) Western blot analysis of actinin-4-depleted HeLa whole-cell lysate. Cells transfected with siRNA directed against actinin-4 were subjected to western blotting. siRNA against luciferase was transfected as a control (non-targeting siRNA). Anti-actinin-1 blotting was performed to check the specificity of the siRNA and anti-α-tubulin serves as a loading control. Ctrl: control (non-targeting siRNA); NT: non-transfected control. (**D**) Immunostaining of HeLa cells and 3T3 cells with #92B, anti-actinin-4 polyclonal antibody and anti-β-actin antibody. Three different localization patterns were observed with #92B and are categorized as strong nucleoplasmic signals (arrows), weak cytoplasmic signals (closed arrowheads), and both nucleoplasmic and cytoplasmic staining (open arrowheads). Scale bars: 10 μm. (**E**) #92B blocking assay with an epitope peptide. HeLa cells were subjected to immunostaining with #92B in the presence of GST-tagged actinin-4 fragment (amino acid residues 287-758). The same concentration of GST peptide was mixed with the antibody as a control. Scale bars: 10 μm.

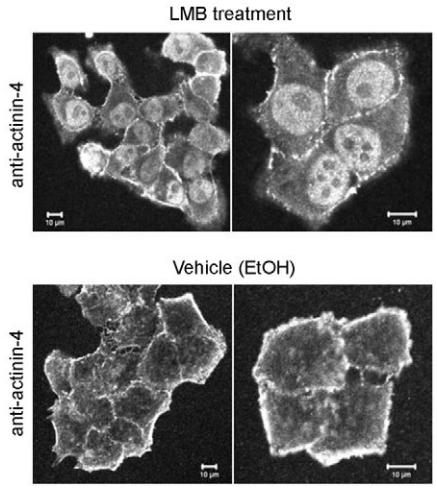

Fig. 2. Actinin-4 accumulates in the nucleus following treatment with LMB. Immunostaining of LMB-treated HeLa cells. The cells were incubated with 5 ng/ml LMB for 24 hours and subjected to immunostaining by anti-actinin-4 polyclonal antibody. The same volume of ethanol (vehicle) was incubated as a control. Scale bars: 10 μm.

adhesions and colocalized with β-actin (Fig. 1D). By contrast, #92B did not colocalize with β-actin and the pattern of immunostaining differed among cells. Some cells demonstrated a strong nuclear signal, some exhibited a complete lack of nuclear signal, whereas others showed a similar level of fluorescent signal in both the nucleoplasm and cytoplasm (Fig. 1D, arrows). These results indicated that #92B recognizes specific forms of actinin-4 that are dissociated from the focal adhesion. When the #92B epitope peptide was used to block antibody binding, both the nuclear and cytoplasmic signals disappeared (Fig. 1E). GST-tagged peptide alone did not affect immunostaining, demonstrating that the immunofluorescent signals of #92B were derived from actinin-4. These results suggested that some actinin-4 is generally localized to the nucleus without any stimulation. Nuclear localization of actinin-4 was also observed in mouse 3T3 cells (Fig. 1D). Thus, it appears likely that nuclear localization of actinin-4 occurs universally among different cell types and species.

Actinin-4 acts as a nucleocytoplasmic shuttling molecule and contains a functional nuclear export signal

HeLa cells for immunostaining were pretreated with 5 ng/ml leptomycin B (LMB), a specific inhibitor of chromosome region maintenance-1 (CRM1). Under these experimental conditions, nuclear signals were detected when using the anti-actinin-4 polyclonal antibody, but there were no signals in non-treated cells (Fig. 2). Control immunostaining of β-actin (positive) and keratin-8 (negative) was performed to ensure successful LMB treatment (supplementary material Fig. S1). This result indicates that actinin-4 serves as a shuttling molecule between the nucleoplasm and cytoplasm, and that the amount of nuclear actinin-4 is significantly smaller than the amount present in the actin cytoskeleton.

CRM1 is known to mediate nuclear export, which requires the nuclear-export signal (NES). A search for the NES consensus sequence – L-x(2,3)-(L, I, V, F, M)-x(2,3)-(L, I)-x-(L, I) (Bogerd et al., 1996; la Cour et al., 2003) – in the entire actinin-4 molecule revealed two putative NESs at amino acid residues 141-152 and 523-532 (Fig. 3A). The former site is located in the middle of the two CH domains, whereas the latter is positioned in the middle of the SR region (Fig. 3B). To investigate whether these putative NESs are functional, a set of GFP-fused deletion constructs including or excluding the NES was generated (Fig. 3C). Interestingly, the GFP-fused SR region (287-758) dominantly localized to the nucleus, suggesting that this region possesses the potential to migrate into the nucleus. Construct region 152-758 was also dominantly localized to the nucleus, whereas construct 141-758 was found to be successfully excluded from the nucleus. Furthermore, LMB treatment resulted in the nuclear accumulation of full-length and the 141-758 fragment of actinin-4, indicating that the NES at amino acid residues 141-152 is functional (Fig. 3D). These findings were consistent with a previous report demonstrating that a splicing variant of actinin-4 that lacked amino acid residues 89-478 was predominantly localized to the nucleus (Chakraborty et al., 2006). Thus, the nuclear export of actinin-4 appears to be regulated by the NES-dependent, CRM1-mediated nuclear export pathway.

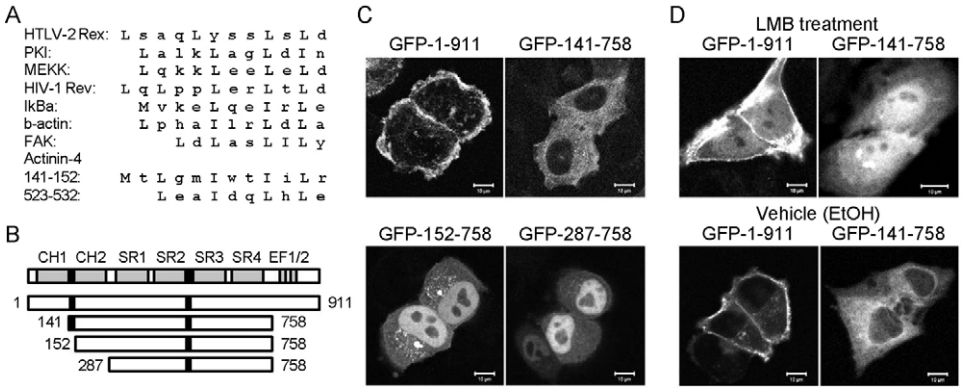

Fig. 3. Actinin-4 contains a functional NES. (**A**) Comparison of known NES and two putative NES sequences from actinin-4. The NES consensus amino acids are indicated in capital letters. (**B**) Schematic model of truncated actinin-4 mutants. Four constructs were designed as follows: amino acids 1-911 (full length); 141-758 (contains two NES sequences); 152-758 (contains one NES); and 287-758 (whole SR region). The two putative NES sequences are indicated by the black boxes. (**C**) Subcellular localization of GFP-fused truncated mutants. HeLa cells were transfected with the constructs and incubated for 24 hours following microscopic observation. Scale bars: 10 μm. (**D**) Nuclear accumulation of GFP-fused full-length actinin-4 and fragment 141-758 in LMB-treated cells. HeLa cells transfected with the GFP constructs were treated with 5 ng/ml LMB for 24 hours and then subjected to microscopic observation. Scale bars: 10 μm.

Actinin-4 interacts with the NPC and independently migrates through the nuclear membrane

Although actinin-4 was found to function as a shuttling molecule, the nuclear-import mechanisms remain unknown. To investigate the molecular mechanism underlying the nuclear import of actinin-4, nuclear-transport assays were performed using semi-intact HeLa cells. These cells were first treated with digitonin, a chemical that exhibits a high affinity for cholesterol and selectively permeabilizes the cell membrane. The cells were then incubated with florescence-fused proteins of interest. Using this system, the addition of IgG conjugated to Alexa-Fluor-568 to the observation buffer labels the nucleus as black spots and indicates whether the nuclear membrane is intact. GFP-fused proteins with NLSs are expected to pass through the NPC. We found that the GST-NLS-GFP protein was transported into the nucleus when incubated with the transport components importin-α, importin-β, RanGDP and the ATP-regeneration system, but not without sufficient transport components (Fig. 4A). By contrast, the GFP-fused actinin-4 SR region (287-758), which has a molecular mass of 87 kDa and shows nuclear localization in vivo (Fig. 3C), exhibited nuclear localization in the presence and absence of transport components (Fig. 4B).

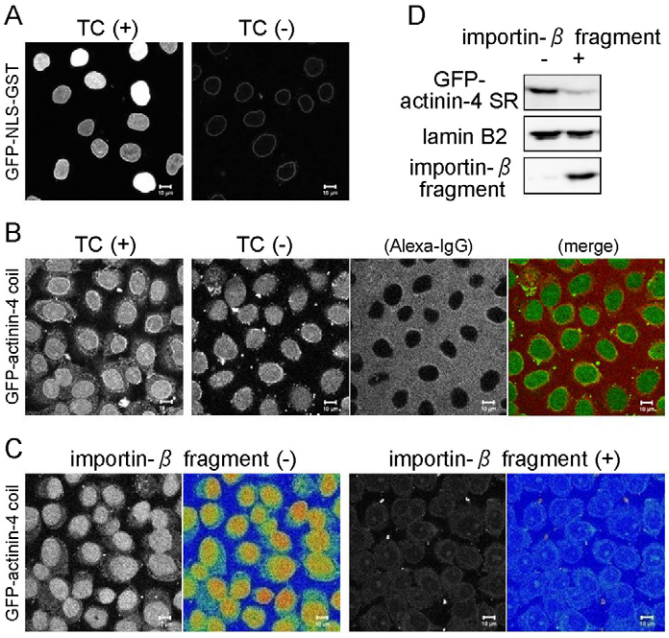

Fig. 4. SR region of actinin-4 interacts with the NPC and passes through the nuclear membrane independently. (**A**) Nuclear-transport assay using a control GFP-NLS-GST peptide. HeLa cells were semi-permeabilized with digitonin and incubated with the transport substrate for 30 minutes. GFP signals were observed in the nucleus when the substrate contained the transport components (importin-α, importin-β, RanGDP and the ATP-regeneration system), but were not observed in their absence. TC: transport components. Scale bars: 10 μm. (**B**) Nuclear-transport assay using a GFP-fused peptide corresponding to the actinin-4 SR region (amino acids 287-758). The peptide was purified from bacterial expression. Alexa-Fluor-568-conjugated IgG was added to the solution to reveal the intact nuclear membrane. Scale bars: 10 μm. (**C**) The inhibitory effects of an importin-β fragment on the nuclear transport of actinin-4. Semi-permeabilized cells were preincubated with an importin-β fragment (amino acids 45-462) that blocks FG-Nups in the NPC and then applied to the assay. Gray scale images (left) and rainbow-scale images (right). Scale bars: 10 μm. (**D**) Western blot analysis of the transported peptide. Cells were collected after the transport assay with or without importin-β fragment, and subjected to western blot analysis. The transported GFP–actinin-4 peptide was detected using anti-GFP antibody.

The molecular mechanisms underlying importin-dependent nuclear transport are known to rely on the hydrophobic interaction between the NPC and its associated proteins. Importin-β contains numerous hydrophobic helices and two consecutive α-helices form several pockets that directly interact with the phenylalanine-glycine (FG)-motif-containing proteins (or FG-Nups) in the NPC (Otsuka et al., 2008; Patel et al., 2007). This direct interaction between the hydrophobic helix and the FG-motif is thought to be responsible for the migration of this molecule through the NPC. The importin-β fragment containing amino acids 45-462 has been shown to lack both the N-terminal Ran-binding site and the C-terminal cargo-binding site, binds tightly to the NPC, masks the interactive FG-motif of the FG-Nups and thus inhibits FG-mediated nuclear transport (Kutay et al., 1997). When the semi-intact cells were pretreated with the importin-β 45-462 fragment, nuclear accumulation of the GFP-fused actinin-4 SR region was effectively inhibited (Fig. 4C). Western blot analysis of the transported materials also demonstrated that the levels of transported actinin-4 peptide were significantly decreased in the presence of the importin-β fragment (Fig. 4D). Given these results, we conclude that the nuclear import of actinin-4 is mediated by its inner SR region and the molecule clearly passes through the NPC.

Localization and biochemical properties of actinin-4 are significantly altered during cell-cycle progression

HeLa cells were synchronized using the double-thymidine block method and subjected to immunostaining with #92B at specific time intervals following release (Fig. 5A). We counted more than 600 cells and classified them into three localization pattern categories: nucleoplasmic localization; cytoplasmic localization; and localization at both sites (Fig. 1, arrows). The histogram illustrates the alterations in the nucleoplasm-localized population during the cell cycle (Fig. 5B). Approximately 10% of the nuclear population was found to be in the S phase. This number increased significantly to 80% in the G2 phase, before gradually decreasing in the G1 phase. Synchronization was assessed by means of changes in cyclin E levels and the total amount of actinin-4 remained constant throughout the cell cycle (Fig. 5C). Given that there were no obvious band shifts in the western blot using #92B and the anti-actinin-4 polyclonal antibody, the changes in localization were most probably not due to either protein digestion or degradation.

The subcellular fractionation technique was developed to separate proteins based on their biochemical properties (Fey et al., 1986). When immunostaining and immunoblotting analyses were undertaken in combination with the fractionation technique, we observed two distinct populations of actinin-4 molecules: a population eluted by high-salt buffer and a highly insoluble population (Fig. 6A,B). Lamin B2 and α-tubulin immunoblotting was performed to assess fractionation. The nuclear actinin-4 recognized by #92B was eluted following high-salt buffer treatment (Fig. 6A), indicating that nuclear actinin-4 possesses different biochemical properties to the highly insoluble cytoskeletal forms of the molecule. Thus, it is suggested that nuclear actinin-4 might play a different role to actinin-4 located at the actin cytoskeleton. When the high-salt extraction was performed on the synchronized G2-phase cells and subjected to western blot analysis, significantly larger amounts of actinin-4 were detected in the extracted fraction compared to the non-synchronized cells (Fig. 6C). The intensity of the non-synchronized bands compared with that of G2-phase cells

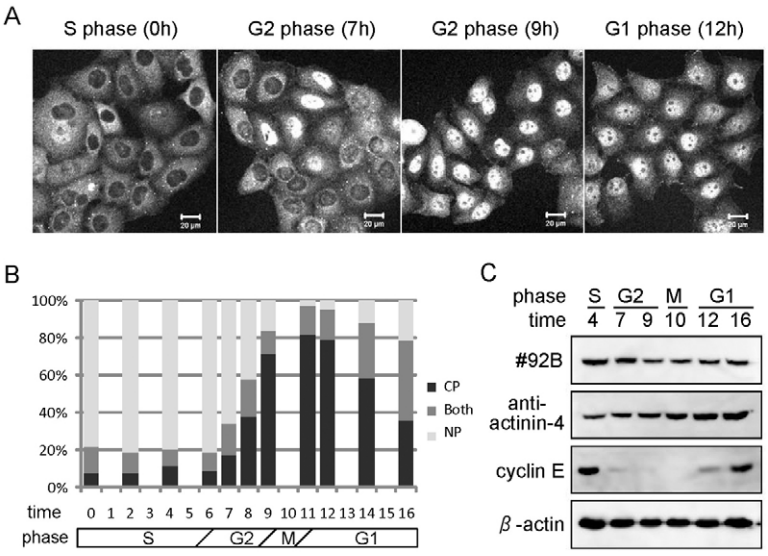

Fig. 5. Nuclear localization of actinin-4 is regulated in a cell-cycle-dependent manner. (**A**) HeLa cells were synchronized to the G1-S phase by double-thymidine block and subjected to immunostaining with #92B at specific time intervals after release. Scale bars: 20 μm. (**B**) Statistical analysis of the signal patterns observed by #92B immunostaining. More than 600 cells in each phase were counted and classified according to the distribution patterns indicated in Fig. 1D. NP: strong nucleoplasmic signal, CP: cytoplasmic signal, both: both nucleoplasmic and cytoplasmic signal. *n*=638 (0 hours), 746 (2 hours), 705 (4 hours), 477 (6 hours), 601 (7 hours), 648 (8 hours), 766 (9 hours), 626 (11 hours), 709 (12 hours), 657 (14 hours), 603 (16 hours). (**C**) Western blot analysis of synchronized HeLa cell lysates. Whole-cell lysates from each indicated cell phase were subjected to western blot analysis using #92B, anti-actinin-4 polyclonal antibody, anti-cyclin E and anti-β-actin.

was estimated at 1:2.5 (Fig. 6D). LMB treatment also resulted in an increase in the high-salt-soluble population (Fig. 6D). As the total actinin-4 levels were unchanged throughout the cell cycle, the increase in the nuclear population was probably due to an increase in the levels of high-salt-soluble actinin-4 in the G2 phase. It is reported that the proteins in different fractions participate in the formation of different orders of architecture in both nucleus and cytoplasm (Yoshimura et al., 2003). Therefore, it is suggested that highly soluble nuclear actinin-4 is not involved in the bundling of actin filaments, as in the cytoplasm, and that actinin-4 is a multifunctional molecule.

Actinin-4 interacts with the INO80 chromatin-remodeling complex

The INO80 chromatin-remodeling complex is a member of the SWI/SNF2 family of ATP-dependent chromatin-remodeling complexes and is composed of Ino80 protein, actin, actin-related protein (Arp) 4, Arp5, Arp8 and RuvB ATPases (Cai et al., 2007; Harata et al., 2000; Jin et al., 2005; Shen et al., 2003). Because the INO80 complex contains many actin cytoskeletal proteins, the molecular interactions and functional relationship between actinin-4 and this complex were analyzed to understand the role of actinin-4 in the nucleus. Full-length cDNA of the human Ino80 protein was cloned and expressed in HeLa cells in a GFP-fused form. The fluorescent signal was mainly observed in the nucleus, demonstrating that the GFP tag did not result in the abnormal localization of Ino80 (supplementary material Fig. S2A). Endogenous Arp5 was also found ubiquitously in the nucleus, whereas nuclear actinin-4 was found in some of the cells, depending on the cell-cycle phase, as we revealed previously (Fig. 7A). Precipitation assays were then undertaken against GFP-Ino80 and the coprecipitated proteins were analyzed by western blot. The coprecipitated fraction contained significant amounts of actinin-4, Arp5 and β-actin (Fig. 7B). The same coprecipitated material immobilized on beads was subjected to binding assays with the bacterially expressed GST-fused actinin-4 fragments. The full-length

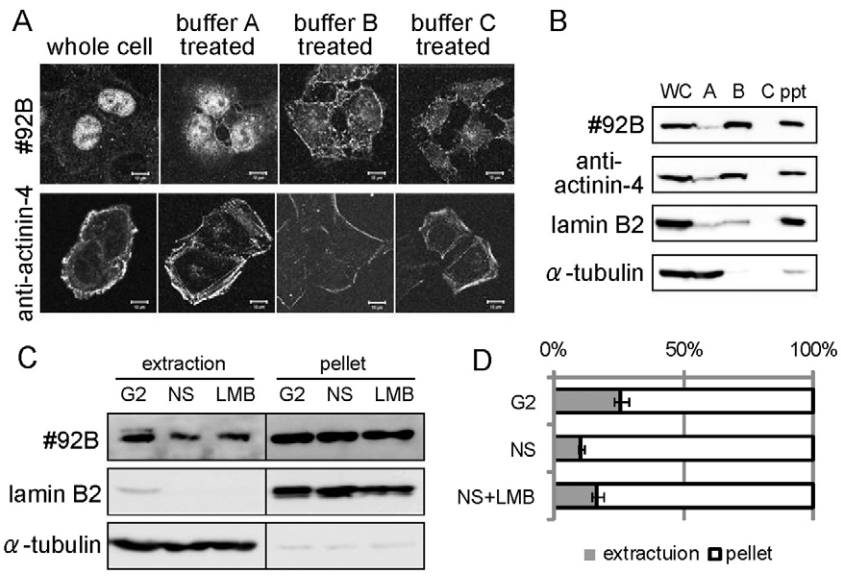

Fig. 6. Localization-dependent and cell-cycle-dependent alteration in the biochemical properties of actinin-4. (**A**) HeLa cells were sequentially treated with detergent buffer (buffer A), high-salt buffer (buffer B) and DNase buffer (buffer C), and subjected to immunostaining with #92B and anti-actinin-4 antibody. Scale bars: 10 μm. (**B**) Western blot analysis of the extracted proteins in each buffer treatment. Actinin-4 was mainly detected in the high-salt buffer fraction and the pellet fraction. Successful fractionation was monitored by anti-lamin B2 and anti-α-tubulin blotting. WC: whole cell, A,B,C: fractions eluted by each buffer treatment, ppt: pellet after the sequential treatment. (**C**) Western blot analysis of proteins extracted by high-salt buffer. The following phases of the cells were directly subjected to buffer B extraction: G2, synchronized to G2 phase by double-thymidine block (8.5 hours after release); NS, non-synchronized control; and LMB, treated with LMB for 24 hours. Both extracted and pellet fractions were subjected to the #92B western blot. The amounts of lamin B2 and α-tubulin were monitored as loading controls. (**D**) Statistical analysis of the western blots. The intensities of the actinin-4 bands were measured and calibrated by the lamin B2 and tubulin bands. Error bars indicate ± s.d. (*n*=3).

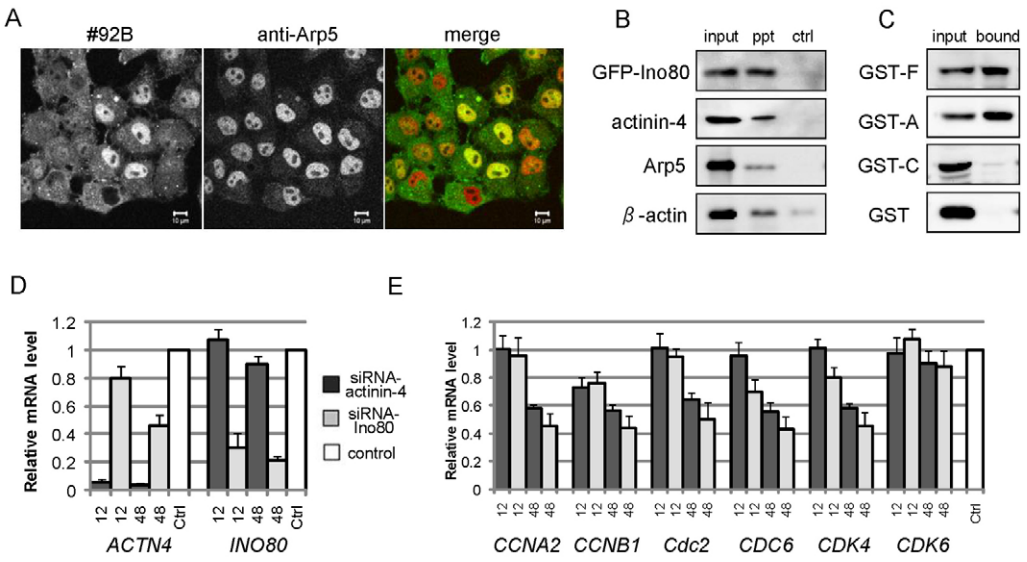

Fig. 7. Actinin-4 interacts with the INO80 chromatin-remodeling complex and is involved in transcriptional regulation. (**A**) Subcellular localization of nuclear actinin-4 and Arp5. Arp5 was ubiquitously localized to the nucleus, whereas the nuclear localization of actinin-4 was observed in particular cells. Green: #92B, red: Arp5. Scale bars: 10 μm. (**B**) Coprecipitation assay of actinin-4 with Ino80. HeLa cells expressing GFP-Ino80 were applied to anti-GFP immunoprecipitation and the coprecipitated materials were analyzed by western blot. Endogenous actinin-4, Arp5 and β-actin were coprecipitated with GFP-Ino80. ppt: precipitated materials, ctrl: precipitation by control IgG. (**C**) Pull-down assay of GST–actinin-4 fragments with the INO80 complex. Purified GST–actinin-4 fragments expressed in bacteria were incubated with GFP-Ino80 complex precipitated from HeLa cells. The bound fractions were analyzed by anti-GST western blot. F: full-length, A: actin-binding region, C: central SR region. (**D**) Gene expression analysis of actinin-4 and Ino80 knockdown cells by quantitative PCR. Total RNA was extracted from HeLa cells 12 or 48 hours after siRNA transfection. siRNA against luciferase was transfected as a non-targeting control siRNA. The amount of 18S rRNA was measured as a loading control. Each column shows the relative mRNA levels of actinin-4 gene (*ACTN4*) and Ino80 gene (*INO80*) normalized by the control. Black columns: actinin-4 knockdown cells, gray columns: Ino80 knockdown cells, white columns: controls. Error bars indicate ± s.d. n=3 from two independent siRNA transfection experiments. (**E**) Relative mRNA levels of a set of cell-cycle-related genes were analyzed by quantitative PCR in the same way as described in D. Specific primer sets for cyclin A2 (*CCNA2*), cyclin B1 (*CCNB1*), *Cdc2*, *CDC6*, *CDK4* and *CDK6* were employed to quantitatively analyze the expression of each gene. *CCNB1* gene expression was significantly suppressed after 12 hours incubation with siRNA directed against actinin-4 (0.73), to the same level as Ino80 knockdown (0.76). *CDC6* and *CDK4* genes were suppressed by Ino80 knockdown, but not affected by actinin-4 knockdown. All the genes examined except *CDK6* were suppressed in both siRNA treatments after 48 hours. Error bars indicate ± s.d. n=3 from two independent siRNA transfection experiments.

molecule and the actin-binding domain of actinin-4 were successfully pulled down by the INO80 complex, whereas the central SR region and the GST tag alone were not detected (Fig. 7C). The actin-binding region is responsible for the actinin-4–INO80 complex interaction, a process that might be mediated by β-actin and Arps.

The functional relationship between actinin-4 and the INO80 complex was then analyzed by focusing on cell-cycle-dependent transcriptional regulation. This complex is known to regulate as much as two-thirds of the total gene expression in yeast, including cell-cycle-related genes such as cyclins and cell-cycle checkpoint factors (Shimada et al., 2008). Total RNA was extracted from HeLa cells 12 or 48 hours following transfection with small interfering (si)RNA directed against actinin-4 or Ino80. The effect of this RNAi system on target mRNA levels was analyzed by quantitative PCR. The actinin-4 gene (*ACTN4*) was effectively suppressed both 12 and 48 hours following incubation with actinin-4 siRNA (relative score: 0.05 and 0.04), whereas Ino80 knockdown resulted in only an approximately 70% reduction in *INO80* expression (0.31 and 0.24) (Fig. 7D). Although the mRNA level of *ACTN4* was slightly affected by Ino80 knockdown, the protein level and the nuclear localization of actinin-4 were not affected within this timeframe (supplementary material Fig. S2B,C). Relative mRNA levels of a set of cell-cycle-related genes were then analyzed, including *CDC6*, which is known to be regulated by the INO80 complex in human cells (Cai et al., 2007). The results of these experiments suggested the involvement of actinin-4 in the expression of cell-cycle-dependent genes. Knockdown of Ino80 resulted in the suppression of *CyclinB1* (*CCNB1*), *CDC6* and *CDK4* after 12 hours (Fig. 7E). Interestingly, actinin-4 knockdown significantly affected *CCNB1* gene expression, but did not affect *CDC6* and *CDK4* after 12 hours, suggesting that actinin-4 affects a subset of INO80-dependent gene expression. After a 48-hour incubation, the vast majority of target genes, except *CDK6*, were negatively regulated by both knockdowns. This result might reflect indirect knockdown effects, including cell-cycle defects. Actinin-4 appeared to regulate specific gene expression in conjunction with the INO80 complex in a cell cycle-dependent manner. *CCNB1* is one of the target genes of the actinin-4-containing INO80 complex.

Actinin-4 associates with the rRNA transcriptional machinery during mitosis

Nuclear actinin-4 exhibited distinct and dynamic behavior during mitosis. HeLa cells stained with #92B demonstrated strong signals located on the condensed mitotic chromosomes (Fig. 8A). It is well established that various rRNA transcription factors, such as RNA polymerase I and upstream binding factor (UBF), form foci on rDNA regions termed nucleolar organizer regions (NORs) of

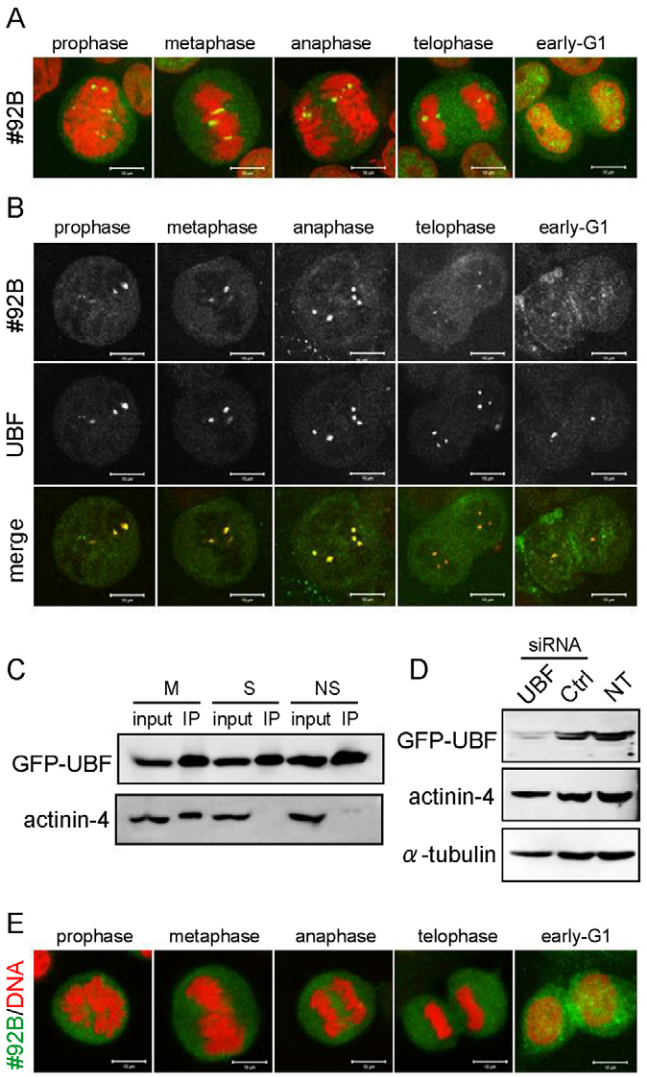

Fig. 8. Actinin-4 localizes to the NOR during mitosis in a UBF-dependent manner. (**A**) Mitotic localization of nuclear actinin-4 on chromosomes revealed by #92B immunostaining. Green: #92B signal, red: DNA stained with PI. Scale bars: 10 μm. (**B**) #92B immunostaining of HeLa cells expressing GFP-UBF. Mitotic colocalization was observed by confocal microscopy. Green: GFP-UBF, red: #92B. Scale bars: 10 μm. (**C**) Coprecipitation analysis of GFP-UBF and actinin-4. HeLa cells expressing GFP-UBF were arrested in M phase or S phase, and subjected to anti-GFP immunoprecipitation. The precipitated materials were analyzed by anti-GFP and anti-actinin-4 immunoblotting. M: sample from M-phase cells, S: S-phase cells, NS: non-synchronized cells, IP: immunoprecipitated fraction. (**D**) Western blot analysis demonstrating the knockdown efficiency of siRNA against UBF. GFP-UBF-expressing HeLa cells were transfected with siRNA against UBF and the whole-cell lysate was subjected to western blot analysis. The efficiency of RNAi was estimated to be 0.27 by anti-GFP blotting compared to α-tubulin. The protein level of actinin-4 was not changed. (**E**) Mitotic observation of actinin-4 in UBF knockdown cells. The siRNA against UBF was transfected into HeLa cells and incubated for 2 days. The nuclear actinin-4 was detected by #92B immunostaining. Scale bars: 10 μm.

specific mitotic chromosomes (Roussel et al., 1996). When the UBF was expressed in a GFP-fused form, the #92B signals completely overlapped with the GFP-UBF foci located on the mitotic chromosomes (Fig. 8B). These results revealed that the actinin-4 foci correspond to the NORs. Both actinin-4 and UBF accumulated in the NORs before prophase and were equally divided into the two daughter cells. When the cells entered telophase, the actinin-4 signals were reduced and more dispersed, whereas the UBF signals remained localized to the NORs until the early G1 phase. The association of actinin-4 with UBF was also assessed via coprecipitation analysis (Fig. 8C). Significant amounts of actinin-4 were coprecipitated with UBF from colcemid-arrested mitotic cell lysate, whereas protein bands were not detected in S-phase or non-synchronized samples. Thus, actinin-4 interacts with the rRNA transcriptional machinery in a mitotic-specific manner.

The suppressive effect of siRNA directed against UBF was monitored by western blot analysis of HeLa cells stably expressing GFP-UBF. Compared to the protein level of α-tubulin, the GFP-UBF protein level decreased to 0.27 (Fig. 8D). The endogenous UBF would also be suppressed to the same level. Although the protein level of actinin-4 detected by the western blot remained unaffected (1.02), the actinin-4 signal localized to the NORs disappeared following siRNA knockdown of UBF (Fig. 8E). Therefore, the localization of actinin-4 on mitotic NORs was UBF dependent. The rRNA transcriptional machinery is known to contain nuclear actin (Philimonenko et al., 2004), suggesting that the association of actinin-4 with this complex might also be mediated by actin or actin-related molecules, as in the case of the INO80 complex.

Discussion

Multifunctional actinin-4 at focal adhesions and the nucleus

In this study, we demonstrated that actinin-4 was localized to the focal adhesions, cytoplasm and nucleoplasm. In addition, polyclonal antibody raised against actinin-4 recognized focal adhesions and the nucleus of LMB-treated cells (Fig. 2). We hypothesized that the actinin-4 polyclonal antibody might recognize all subcellular actinin-4 and therefore reflect the relative levels of the molecules in a cell. The vast majority of the actinin-4 molecules were located at the focal-adhesion sites, whereas reduced levels were identified in the cytoplasm and nucleoplasm. By contrast, monoclonal antibody #92B did not recognize the focal-adhesion form of the actinin-4 molecule (Fig. 1). It is reasonable to assume that the epitope of #92B was masked by factor(s) in the focal adhesion. The #92B epitope exactly matches the VBS, which forms a distinct helix and can bind vinculin both in vivo and in vitro (McGregor et al., 1994; Zhang et al., 2009). A three-dimensional model of the binding of actinin and vinculin showed that the VBS is completely covered by the vinculin molecule (Bois et al., 2005). Combining our results with previous findings, it is likely that vinculin binding masks the #92B epitope and therefore #92B specifically recognizes the vinculin-free form of actinin-4. Alternatively, masking of the #92B epitope might not necessarily be done by vinculin. Although vinculin is the most probable candidate for this, it might also be possible that other factors affect #92B binding to actinin-4, such as dimerization or the binding of other proteins.

Proteomic analysis of the various subcellular structures has been undertaken previously to identify the precise composition of these elements. Three different types of proteomic analyses of the nuclear matrix, nucleolus and mitotic chromosomes revealed that actinin-4 was located within the nuclear matrix and in mitotic chromosomes, but was not found in the nucleolus (Andersen et al., 2002; Hirano et al., 2009; Ishii et al., 2008; Scherl et al., 2002; Uchiyama et al., 2005). These findings are consistent with our observation that

actinin-4 was localized to the NORs during mitosis (Fig. 8), but was not identified within the nucleolus at any stage of interphase cells. Therefore, the association of actinin-4 with the rRNA transcriptional machinery might represent a mitotic-specific event. Nuclear actin and myosin I are known to be associated with various transcriptional elements related to RNA polymerases I, II and III (Hofmann et al., 2004; Hu et al., 2004; Philimonenko et al., 2004). Actinin-4 might exhibit correlative functions with these factors, although its precise role on the NORs remains unclear.

The SR region of actinin-4 possesses the potential to migrate into the nucleus

In this study, we demonstrated that the SR region of actinin-4 itself possesses the potential to migrate into the nucleus through the NPC. Nuclear-transport assays showed that the nuclear import of this protein was mediated by its inner SR region, independent of transport mediators (Fig. 4). We hypothesize that the hydrophobic helices located in the central SR region directly interact with FG-Nups in the NPC. It has been reported previously that binding pockets consisting of two hydrophobic helices present in importin-β directly interact with the FG-motifs of the NPC (Otsuka et al., 2008). Given that the surface-charge-potential distribution of the actinin SR region revealed numerous hydrophobic areas on the surface (Ylanne et al., 2001), the SR region could interact with the NPC in the same manner as importin-β. This leads to our hypothesis that the molecular mechanisms underlying nuclear localization of actinin-4 are dependent on a direct interaction with FG-Nups. The molecular mechanisms underlying karyopherin-independent nuclear import of cytoskeletal proteins over 100 kDa in size have not been reported to date. These mechanisms will also be relevant to other SR-containing structural proteins that are localized to the nucleus.

Molecular mechanisms controlling nuclear levels of actinin-4

Nuclear localization of actinin-4 is thought to be regulated by the balance between nuclear import and export (Fig. 9A). The molecular mechanisms of nuclear import and export have not been elucidated for all kinds of proteins. The rate of nuclear import and export should vary depending upon the protein, and the cytoplasmic and nuclear distribution of a particular protein should be determined from the balance of nuclear import and export. In this sense, it is interesting and important to consider the following facts. First, in the case of focal adhesion kinase (FAK, a 122 kDa protein that contains both NLS and NES), most of the molecules are localized to the focal adhesion, suggesting that the NES is much more powerful than the NLS in this case (Lobo and Zachary, 2000; Ossovskaya et al., 2008; Stewart et al., 2002). Second, the GFP-fused actinin-4 141-758 fragment (which contains NES and SR) did not localize to the nucleus (Figs 3, 4). When the cells were treated with LMB for 4 hours, significant accumulation of the FAK protein in the nucleus was observed. By contrast, it was difficult to detect a nuclear signal under the same conditions following incubation with the anti-actinin-4 polyclonal antibody (data not shown). These findings suggest that the SR-dependent nuclear import of actinin-4 appeared to be very slow compared to NLS-dependent transport, and the NES-dependent nuclear export of actinin-4 is much more powerful than nuclear import. Alternatively, it is also possible that actinin-4 exhibits a high affinity for actin-related cytoskeletons and has more limited opportunities to reach the NPC.

Considering the molecular mechanisms underlying nuclear import and export, there are two possible ways in which the nuclear localization of actinin-4 is regulated. One way is through the regulation of CRM1 activity levels. As actinin-4 is exported in an NES-dependent manner, CRM1 might directly regulate the nuclear localization of actinin-4. It has been reported that the expression of mammalian CRM1 is initiated in the late G1 phase and reaches its peak at the G2-M phase. However, the total protein levels remain unchanged throughout the cell cycle (Kudo et al., 1997). This result suggests that the overall activity of CRM1 does not change during the cell cycle and thus nuclear export of actinin-4 would remain constant. Another way in which nuclear localization of actinin-4

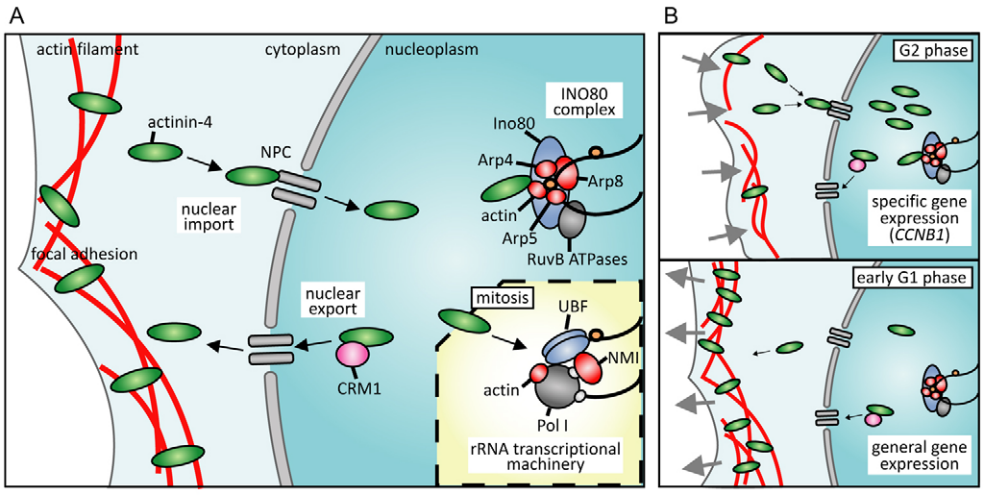

Fig. 9. Schematic diagram of actinin-4 dynamics. (**A**) A model of subcellular actinin-4 dynamics. Actinin-4 molecules interact with NPC component(s) and independently enter the nucleus. The NES sequence is recognized by CRM1 and the molecule is exported from the nucleus. In the nucleus, actinin-4 associates with the INO80 chromatin-remodeling complex and regulates cell-cycle-dependent gene expression. Actinin-4 also interacts with the rRNA transcriptional machinery in a stage-specific manner during mitosis. (**B**) A model of cell-cycle-dependent changes following alterations in nuclear actinin-4 levels. Shrinkage of the cell in the G2 phase promotes the release of actinin-4 from the actin cytoskeleton and results in an increase in nuclear actinin-4 molecules (upper panel). During the early G1 phase, expansion of the cell followed by active construction of the actin cytoskeleton results in a decrease in both cytoplasmic free actinin-4 and nuclear actinin-4 (lower panel).

might be regulated is through the release of actinin-4 molecules from the cytoskeleton. As the actinin-4 molecule itself possesses nuclear-import potential, an increase in the level of free molecules might directly accelerate nuclear import. In combination with our cell-cycle observations and high-salt extraction analyses, the nuclear population in the G2 phase reasonably becomes greater because of an increase in the number of free molecules during this phase (Fig. 9B). It has been reported that the amount of the focal-adhesion protein paxilin is significantly reduced during mitosis, whereas the amount of other focal-adhesion proteins remained constant. That is, focal-adhesion components appear to behave differently during mitotic events (Yamaguchi et al., 1997). As actinins function to anchor F-actin to the focal adhesions, it is likely that degradation of various focal-adhesion components might induce the release of actinin-4 from the cytoskeletal architecture and result in an increase in nuclear actinin-4 levels.

Actinin-4 as a link between cytoskeleton and gene expression

Our studies revealed the molecular mechanisms underlying the nucleocytoplasmic shuttling of actinin-4 and its role in the expression of cell-cycle-dependent genes. We hypothesize that this molecular shuttling serves as a link between morphological changes in the cytoskeleton and cell-cycle-dependent gene expression, and is important for the orchestration of cell activity (Fig. 9). Nuclear actin and Arps have been identified in several chromatin-remodeling complexes, where they are thought to play key roles in the transcriptional regulation of numerous genes (Hofmann et al., 2004; Hu et al., 2004). The rRNA transcriptional machinery also contains nuclear actin and myosin I (Philimonenko et al., 2004). It therefore seems likely that nuclear transcriptional events are dynamically regulated by cytoskeletal components. Actinin-4 might also play an important role in transcriptional regulation. Indeed, a splicing variant of actinin-4 that lacks amino acid sequence 89-478 is predominantly localized to the nucleus and mediates the transcription of the *TAF55* gene, which is regulated by myocyte enhancer factor-2 (Chakraborty et al., 2006). In this study, we showed that nuclear actinin-4 associates with the INO80 chromatin-remodeling complex via its actin-binding domain, an association that directs the expression of a subset of cell-cycle-dependent genes. It appears reasonable that actinin-4 is associated with various chromatin-remodeling complexes, as all of the SWI/SNF-like complexes examined to date contain at least one actin or Arp isoform (Szerlong et al., 2008). These findings suggest a more general role for nuclear actinin-4 in transcriptional regulation, in addition to other actin cytoskeletal proteins in the remodeling complex.

Because the expression of the M-phase cyclin *CCNB1* gene was rapidly suppressed in actinin-4 knockdown cells, *CCNB1* might serve as a direct target gene of the actinin-4-containing INO80 complex. A global gene expression analysis of a yeast strain lacking *INO80* revealed that various cell-cycle-related genes are regulated by the INO80 complex (van Attikum et al., 2004). In this strain, the expression of the M-phase cyclins *CLB1-CLB4* was most significantly affected among all the cyclin genes, a finding that was consistent with our results in human cells. Considering the facts that nuclear actinin-4 was observed only in particular cells, whereas Ino80 and Arp5 were localized to the nucleus ubiquitously, some cells are likely to contain actinin-4-containing INO80 complexes, others actinin-4-depleted INO80 complexes (Fig. 9B). We hypothesize that the actinin-4-containing INO80 complex is responsible for specific gene expression in late-G2 to early-G1 phase.

Although we revealed the functional interactions of actinin-4 with transcriptional regulators, actinin-4 knockdown did not result in phenotypic defects, such as growth inhibition, abnormal morphology and mitotic defects. The actinin-4 knockdown cells grow as well as cells transfected with a non-targeting siRNA for up to 48 hours (data not shown). It has been reported that knockdown of Arp5 did not affect cellular proliferation (Kitayama et al., 2009). Because actinin-dependent gene expression is regulated in a tissue-specific manner, nuclear actinin-4 might play an important role in the differentiation process. The precise roles of actinin-4 in cell differentiation require further investigation.

Materials and Methods

Antibodies and cDNA constructions

A monoclonal antibody against actinin-4 (#92B) was obtained by mass production of monoclonal antibodies against nuclear structural proteins (web database: http://www.lif.kyoto-u.ac.jp/labs/chrom/abgallery/index.html). Other antibodies used were: anti-β-actin (Sigma), anti-actinin-4 (ImmunoGlobe), anti-cyclin E (BD Bioscience), anti-α-tubulin (Sigma), anti-GST (Sigma), anti-GFP (MBL). The antibody for Arp5 was raised against human Arp5 (Kitayama et al., 2009). Total RNA was purified from HeLa cells using the RNeasy Midi Kit (Qiagen). The first strand synthesis was performed using the SuperScript First-Strand Synthesis System for reverse-transcription PCR (Invitrogen) according to the manufacturer's protocol. Using this cDNA pool as a template, the following cDNAs for actinin-4 were amplified by PCR and subcloned into pGEX-5X (Amersham Biosciences), pRSET (Invitrogen) and pEGFP-C (Clontech) vectors: full length (amino acid residues 1-911), actin-binding region (1-286), SR region (287-758), SRΔC23 region (287-735), EF-hand region (759-911), NES plus CH2 domain plus SR region (141-758), CH2 domain plus SR region (152-758), and actinin-1 SR region (506-739). The cDNA for the Ino80 protein was purchased from Kazusa DNA Research Institute (KIAA1259). The construct for GFP-fused UBF was a kind gift from Mitsuru Okuwaki, Tsukuba University, Japan.

Cell culture and subcellular fractionation of HeLa cells

HeLa S3 cells and mouse 3T3 cells were cultured in complete Dulbecco's Modified Eagle's Medium (Sigma) supplemented with 10% fetal bovine serum (Hyclone) in 5% CO_2 at 37°C. The basic method was described previously (Fey et al., 1986). For microscopical observations, cells grown on cover glass were washed twice with ice-cold PBS and then incubated with buffer A [10 mM PIPES-NaOH (pH 6.8), 100 mM NaCl, 300 mM sucrose, 3 mM $MgCl_2$, 1 mM EGTA, 0.5% Triton X-100, 1 mM PMSF and 1:100 protease inhibitor cocktail (Nacalai Tesque)] at 4°C for 10 minutes. The cells were then subjected to brief treatment with buffer B [10 mM PIPES-NaOH (pH 6.8), 250 mM $(NH_4)_2SO_4$, 300 mM sucrose, 3 mM $MgCl_2$, 1 mM EGTA, 0.5% Triton X-100, 1 mM PMSF and 1:100 protease inhibitor cocktail (Nacalai Tesque)] at 4°C for 5 minutes. The resulting materials were digested with 10 U/μl DNase I in buffer C [10 mM PIPES-NaOH (pH 6.8), 50 mM NaCl, 300 mM sucrose, 3 mM $MgCl_2$, 1 mM EGTA, 0.5% Triton X-100, 1 mM PMSF and 1:100 protease inhibitor cocktail (Nacalai Tesque)] at 4°C for 30 minutes and then washed with buffer B. For western blot, all the steps were performed in a tube on ice. Each buffer was collected by centrifugation at 700 ***g*** for 2 minutes and used for SDS-PAGE.

Synchronization of HeLa cells

The synchronization was performed by double-thymidine block or by colcemid treatment. For the double-thymidine block, 24 hours after plating the cells, medium containing 2 mM thymidine (Sigma) was supplied. The cells were arrested for 12 hours and then released by providing fresh medium containing 24 μM deoxycytidine for 9 hours. The arrest and release steps were repeated, and the synchronized cells were applied to further assays at intervals after final release. For collecting mitotic cells, colcemid arrest was combined with thymidine block. 0.1 μg/μl colcemid (Nacalai Tesque) was added to the thymidine-synchronized cells and mitotic cells were collected after 3-6 hours.

Immunostaining and microscopical observations

Non-treated, fractionated or LMB-treated (5 ng/ml; Calbiochem) HeLa cells were washed twice by PBS and then fixed with 4% paraformaldehyde in PBS at room temperature for 15 minutes. The samples were blocked with 5% normal goat serum for 15 minutes and then incubated with the first antibody. In the case of non-treated cells, 0.5% Triton X-100 was added to the blocking buffer for permeabilization. Specific binding was detected by fluorescein isothiocyanate (FITC)-conjugated anti-mouse IgG (Cappel Laboratories) or anti-rabbit IgG (Cappel Laboratories). If necessary, the sample was stained with 4,6-diamidino-2-phenylindole (DAPI) or propidium iodide (PI) (final concentration 5 μg/ml) in the mounting medium (Vectashield). Microscopical observations were performed at room temperature using a confocal laser-scanning microscope (LSM 5 PASCAL, Carl Zeiss) with ×63 Plan-Apo objective lens N.A.=1.4.

Nuclear-import assay

The basic method was described previously (Gorlich et al., 1996; Gorlich et al., 1995). The cDNA for the actinin-4 SR region (287-758) was expressed in BL21 *Escherichia coli* cells in GFP-His-tag fused form and purified by Ni-NTA agarose (Qiagen) according to the manufacturer's protocol. HeLa cells were washed twice by ice-cold transport buffer [TB; 20 mM HEPES (pH 7.3), 110 mM potassium acetate, 5 mM sodium acetate, 2 mM magnesium acetate, 1 mM EGTA, 2 mM DTT and 1:100 protease inhibitor cocktail (Nacalai Tesque)] and permeabilized by TB containing 40 μg/ml digitonin for 5 minutes on ice. The cells were washed twice with ice-cold TB and then incubated with TB for 10 minutes on ice. Then, the semi-intact cells were incubated with transport samples (2 μM GFP–His–actinin-4–SR protein with or without 4 μM importin-α, 4 μM importin-β, 25 mM RanGDP, 1 mM ATP, 5 mM creatine phosphate and 20 U/ml creatine phosphokinase) in TB and incubated for 30 minutes at 37°C. The sample was washed twice by ice-cold TB and fixed by 4% paraformaldehyde in TB at room temperature for 15 minutes, and washed twice by TB. Finally, the sample was subjected to immunofluorescence microscopy with TB containing Alexa-Fluor-568-conjugated IgG as a marker for intact cells.

Immunoprecipitation

The cells were resuspended in lysis buffer [20 mM HEPES (pH 7.4), 120 mM NaCl, 5 mM $MgCl_2$, 2 mM EGTA, 1 mM DTT and 1:100 protease inhibitor cocktail (Nacalai Tesque)], sonicated and incubated in the presence of 1% Triton X-100 at 4°C for 20 minutes. After centrifugation at 2000 ***g*** for 20 minutes, the supernatant was collected and incubated with 30 μl anti-GFP-antibody conjugated beads (Nacalai Tesque) at 4°C for 1 hour. The beads were collected by centrifugation, washed five times with lysis buffer, and applied to SDS-PAGE followed by western blot detection.

siRNA-directed gene silencing

RNAi siRNAs were purchased from Invitrogen (Stealth RNAi): actinin-1 (HSS100130), actinin-4 (HSS100123), Ino80 (HSS123095), UBF (HSS111142), with luciferase (12935-146) as a control. siRNAs were transfected with Lipofectamine 2000 (Invitrogen) according to the manufacturer's protocol.

Reverse transcription and quantitative PCR

Cells from a 60 mm culture dish were lysed and total RNA was extracted using the RNeasy Mini Kit (QIAGEN). 2 μg of total RNA was used as a template for reverse transcription by the SuperScript II RT Kit, according to the manufacturer's protocol (Invitrogen). The amount of target cDNA was analyzed by the LightCycler 480 qPCR system (Roche) using FastStart DNA Master SYBR Green kit (Roche) or Thunderbird qPCR mix (TOYOBO). The primer sets used for quantitative PCR were as follows. ACTN4: 5′-TTCAACCACTTCGACAAGGA (forward), 5′-ATGAGGCAGGC-CTTGAACT (reverse); Ino80: 5′-GACGACGAAGAGTTGGAGAAG (forward), 5′-TTCACTCGGTTGGTTTCCTC (reverse); 18S rRNA: 5′-GGAGAGGGAGCCT-GAGAAAC (forward), 5′-TCGGGAGTGGGTAATTTGC (reverse); CCNA2: 5′-CCATACCTCAAGTATTTGCCATC (forward), 5′-TCCAGTCTTTCGTATTAAT-GATTCAG (reverse); CCNB1: 5′-CATGGTGCACTTTCCTCCTT (forward), 5′-AG-GTAATGTTGTAGAGTTGGTGTCC (reverse); CCNE2: 5′-ACCACTTCAATG-GAGGTAAAATG (forward), 5′-GGAAACATTCATTCAAATAGCTCA (reverse); Cdc2: 5′-TGGATCTGAAGAAATACTTGGATTCTA (forward), 5′-CAATCCCCT-GTAGGATTTGG (reverse); CDC6: 5′-CAAAGCTGGTCCTGAACACA-3′ (forward), 5′-TGACATCCATCTCCCTTTCC-3′ (reverse); CDK2: 5′-CCTC-CTGGGCTGCAAATA (forward), 5′-CAGAATCTCCAGGGAATAGGG (reverse); CDK4: 5′-GAGGAGTCGGGAGCACAG (forward), 5′-CTCCGGATTAC-CTTCATCCTT (reverse); CDK6: 5′-TGATCAACTAGGAAAAATCTTGGA (forward), 5′-GGCAACATCTCTAGGCCAGT (reverse); TAF55: 5′-AAAGGAG-GCAGAAAATCAAGG (forward), 5′-CCCTGCCTGTGACCAGAC (reverse).

This work was supported by a Grant-in-Aid for Scientific Research on Priority Areas (to K.T.) from the Ministry of Education, Culture, Sports, Science and Technology of Japan. M.K. was supported by a predoctoral fellowship from the Japanese Society for the Promotion of Science (JSPS).

Supplementary material available online at
http://jcs.biologists.org/cgi/content/full/123/7/1020/DC1

References

Andersen, J. S., Lyon, C. E., Fox, A. H., Leung, A. K., Lam, Y. W., Steen, H., Mann, M. and Lamond, A. I. (2002). Directed proteomic analysis of the human nucleolus. *Curr. Biol.* **12**, 1-11.

Araki, N., Hatae, T., Yamada, T. and Hirohashi, S. (2000). Actinin-4 is preferentially involved in circular ruffling and macropinocytosis in mouse macrophages: analysis by fluorescence ratio imaging. *J. Cell Sci.* **113**, 3329-3340.

Babakov, V. N., Petukhova, O. A., Turoverova, L. V., Kropacheva, I. V., Tentler, D. G., Bolshakova, A. V., Podolskaya, E. P., Magnusson, K. E. and Pinaev, G. P. (2008). RelA/NF-kappaB transcription factor associates with alpha-actinin-4. *Exp. Cell Res.* **314**, 1030-1038.

Beggs, A. H., Byers, T. J., Knoll, J. H., Boyce, F. M., Bruns, G. A. and Kunkel, L. M. (1992). Cloning and characterization of two human skeletal muscle alpha-actinin genes located on chromosomes 1 and 11. *J. Biol. Chem.* **267**, 9281-9288.

Bogerd, H. P., Fridell, R. A., Benson, R. E., Hua, J. and Cullen, B. R. (1996). Protein sequence requirements for function of the human T-cell leukemia virus type 1 Rex nuclear export signal delineated by a novel in vivo randomization-selection assay. *Mol. Cell. Biol.* **16**, 4207-4214.

Bois, P. R., Borgon, R. A., Vonrhein, C. and Izard, T. (2005). Structural dynamics of alpha-actinin-vinculin interactions. *Mol. Cell. Biol.* **25**, 6112-6122.

Bois, P. R., O'Hara, B. P., Nietlispach, D., Kirkpatrick, J. and Izard, T. (2006). The vinculin binding sites of talin and alpha-actinin are sufficient to activate vinculin. *J. Biol. Chem.* **281**, 7228-7236.

Cai, Y., Jin, J., Yao, T., Gottschalk, A. J., Swanson, S. K., Wu, S., Shi, Y., Washburn, M. P., Florens, L., Conaway, R. C. et al. (2007). YY1 functions with INO80 to activate transcription. *Nat. Struct. Mol. Biol.* **14**, 872-874.

Chakraborty, S., Reineke, E. L., Lam, M., Li, X., Liu, Y., Gao, C., Khurana, S. and Kao, H. Y. (2006). Alpha-actinin 4 potentiates myocyte enhancer factor-2 transcription activity by antagonizing histone deacetylase 7. *J. Biol. Chem.* **281**, 35070-35080.

Davison, M. D. and Critchley, D. R. (1988). alpha-Actinins and the DMD protein contain spectrin-like repeats. *Cell* **52**, 159-160.

Fey, E. G., Krochmalnic, G. and Penman, S. (1986). The nonchromatin substructures of the nucleus: the ribonucleoprotein (RNP)-containing and RNP-depleted matrices analyzed by sequential fractionation and resinless section electron microscopy. *J. Cell Biol.* **102**, 1654-1665.

Gorlich, D., Vogel, F., Mills, A. D., Hartmann, E. and Laskey, R. A. (1995). Distinct functions for the two importin subunits in nuclear protein import. *Nature* **377**, 246-248.

Gorlich, D., Pante, N., Kutay, U., Aebi, U. and Bischoff, F. R. (1996). Identification of different roles for RanGDP and RanGTP in nuclear protein import. *EMBO J.* **15**, 5584-5594.

Harata, M., Oma, Y., Tabuchi, T., Zhang, Y., Stillman, D. J. and Mizuno, S. (2000). Multiple actin-related proteins of Saccharomyces cerevisiae are present in the nucleus. *J. Biochem.* **128**, 665-671.

Hirano, Y., Ishii, K., Kumeta, M., Furukawa, K., Takeyasu, K. and Horigome, T. (2009). Proteomic and targeted analytical identification of BXDC1 and EBNA1BP2 as dynamic scaffold proteins in the nucleolus. *Genes Cells* **14**, 155-166.

Hofmann, W. A., Stojiljkovic, L., Fuchsova, B., Vargas, G. M., Mavrommatis, E., Philimonenko, V., Kysela, K., Goodrich, J. A., Lessard, J. L., Hope, T. J. et al. (2004). Actin is part of pre-initiation complexes and is necessary for transcription by RNA polymerase II. *Nat. Cell Biol.* **6**, 1094-1101.

Honda, K., Yamada, T., Endo, R., Ino, Y., Gotoh, M., Tsuda, H., Yamada, Y., Chiba, H. and Hirohashi, S. (1998). Actinin-4, a novel actin-bundling protein associated with cell motility and cancer invasion. *J. Cell Biol.* **140**, 1383-1393.

Hu, P., Wu, S. and Hernandez, N. (2004). A role for beta-actin in RNA polymerase III transcription. *Genes Dev* **18**, 3010-3015.

Imamura, M., Sakurai, T., Ogawa, Y., Ishikawa, T., Goto, K. and Masaki, T. (1994). Molecular cloning of low-Ca(2+)-sensitive-type non-muscle alpha-actinin. *Eur. J. Biochem.* **223**, 395-401.

Ishii, K., Hirano, Y., Araki, N., Oda, T., Kumeta, M., Takeyasu, K., Furukawa, K. and Horigome, T. (2008). Nuclear matrix contains novel WD-repeat and disordered-region-rich proteins. *FEBS Lett.* **582**, 3515-3519.

Jin, J., Cai, Y., Yao, T., Gottschalk, A. J., Florens, L., Swanson, S. K., Gutierrez, J. L., Coleman, M. K., Workman, J. L., Mushegian, A. et al. (2005). A mammalian chromatin remodeling complex with similarities to the yeast INO80 complex. *J. Biol. Chem.* **280**, 41207-41212.

Kitayama, K., Kamo, M., Oma, Y., Matsuda, R., Uchida, T., Ikura, T., Tashiro, S., Ohyama, T., Winsor, B. and Harata, M. (2009). The human actin-related protein hArp5: nucleo-cytoplasmic shuttling and involvement in DNA repair. *Exp. Cell Res.* **315**, 206-217.

Kudo, N., Khochbin, S., Nishi, K., Kitano, K., Yanagida, M., Yoshida, M. and Horinouchi, S. (1997). Molecular cloning and cell cycle-dependent expression of mammalian CRM1, a protein involved in nuclear export of proteins. *J. Biol. Chem.* **272**, 29742-29751.

Kutay, U., Izaurralde, E., Bischoff, F. R., Mattaj, I. W. and Gorlich, D. (1997). Dominant-negative mutants of importin-beta block multiple pathways of import and export through the nuclear pore complex. *EMBO J.* **16**, 1153-1163.

la Cour, T., Gupta, R., Rapacki, K., Skriver, K., Poulsen, F. M. and Brunak, S. (2003). NESbase version 1.0: a database of nuclear export signals. *Nucleic Acids Res.* **31**, 393-396.

Lobo, M. and Zachary, I. (2000). Nuclear localization and apoptotic regulation of an amino-terminal domain focal adhesion kinase fragment in endothelial cells. *Biochem. Biophys. Res. Commun.* **276**, 1068-1074.

McGregor, A., Blanchard, A. D., Rowe, A. J. and Critchley, D. R. (1994). Identification of the vinculin-binding site in the cytoskeletal protein alpha-actinin. *Biochem. J.* **301**, 225-233.

Millake, D. B., Blanchard, A. D., Patel, B. and Critchley, D. R. (1989). The cDNA sequence of a human placental alpha-actinin. *Nucleic Acids Res.* **17**, 6725.

Mimura, N. and Asano, A. (1987). Further characterization of a conserved actin-binding 27-kDa fragment of actinogelin and alpha-actinins and mapping of their binding sites on the actin molecule by chemical cross-linking. *J. Biol. Chem.* **262**, 4717-4723.

Nikolopoulos, S. N., Spengler, B. A., Kisselbach, K., Evans, A. E., Biedler, J. L. and Ross, R. A. (2000). The human non-muscle alpha-actinin protein encoded by the ACTN4 gene suppresses tumorigenicity of human neuroblastoma cells. *Oncogene* **19**, 380-386.

Ossovskaya, V., Lim, S. T., Ota, N., Schlaepfer, D. D. and Ilic, D. (2008). FAK nuclear export signal sequences. *FEBS Lett.* **582**, 2402-2406.

Otey, C. A. and Carpen, O. (2004). Alpha-actinin revisited: a fresh look at an old player. *Cell Motil. Cytoskeleton* **58**, 104-111.

Otsuka, S., Iwasaka, S., Yoneda, Y., Takeyasu, K. and Yoshimura, S. H. (2008). Individual binding pockets of importin-beta for FG-nucleoporins have different binding properties and different sensitivities to RanGTP. *Proc. Natl. Acad. Sci. USA* **105**, 16101-16106.

Patel, S. S., Belmont, B. J., Sante, J. M. and Rexach, M. F. (2007). Natively unfolded nucleoporins gate protein diffusion across the nuclear pore complex. *Cell* **129**, 83-96.

Philimonenko, V. V., Zhao, J., Iben, S., Dingova, H., Kysela, K., Kahle, M., Zentgraf, H., Hofmann, W. A., de Lanerolle, P., Hozak, P. et al. (2004). Nuclear actin and myosin I are required for RNA polymerase I transcription. *Nat. Cell Biol.* **6**, 1165-1172.

Roussel, P., Andre, C., Comai, L. and Hernandez-Verdun, D. (1996). The rDNA transcription machinery is assembled during mitosis in active NORs and absent in inactive NORs. *J. Cell Biol.* **133**, 235-246.

Scherl, A., Coute, Y., Deon, C., Calle, A., Kindbeiter, K., Sanchez, J. C., Greco, A., Hochstrasser, D. and Diaz, J. J. (2002). Functional proteomic analysis of human nucleolus. *Mol. Biol. Cell* **13**, 4100-4109.

Shen, X., Ranallo, R., Choi, E. and Wu, C. (2003). Involvement of actin-related proteins in ATP-dependent chromatin remodeling. *Mol. Cell* **12**, 147-155.

Shimada, K., Oma, Y., Schleker, T., Kugou, K., Ohta, K., Harata, M. and Gasser, S. M. (2008). Ino80 chromatin remodeling complex promotes recovery of stalled replication forks. *Curr. Biol.* **18**, 566-575.

Sjoblom, B., Salmazo, A. and Djinovic-Carugo, K. (2008). Alpha-actinin structure and regulation. *Cell Mol. Life Sci.* **65**, 2688-2701.

Stewart, A., Ham, C. and Zachary, I. (2002). The focal adhesion kinase amino-terminal domain localises to nuclei and intercellular junctions in HEK 293 and MDCK cells independently of tyrosine 397 and the carboxy-terminal domain. *Biochem. Biophys. Res. Commun.* **299**, 62-73.

Szerlong, H., Hinata, K., Viswanathan, R., Erdjument-Bromage, H., Tempst, P. and Cairns, B. R. (2008). The HSA domain binds nuclear actin-related proteins to regulate chromatin-remodeling ATPases. *Nat. Struct. Mol. Biol.* **15**, 469-476.

Uchiyama, S., Kobayashi, S., Takata, H., Ishihara, T., Hori, N., Higashi, T., Hayashihara, K., Sone, T., Higo, D., Nirasawa, T. et al. (2005). Proteome analysis of human metaphase chromosomes. *J. Biol. Chem.* **280**, 16994-17004.

van Attikum, H., Fritsch, O., Hohn, B. and Gasser, S. M. (2004). Recruitment of the INO80 complex by H2A phosphorylation links ATP-dependent chromatin remodeling with DNA double-strand break repair. *Cell* **119**, 777-788.

Virel, A. and Backman, L. (2004). Molecular evolution and structure of alpha-actinin. *Mol. Biol. Evol.* **21**, 1024-1031.

Yamaguchi, R., Mazaki, Y., Hirota, K., Hashimoto, S. and Sabe, H. (1997). Mitosis specific serine phosphorylation and downregulation of one of the focal adhesion protein, paxillin. *Oncogene* **15**, 1753-1761.

Ylanne, J., Scheffzek, K., Young, P. and Saraste, M. (2001). Crystal structure of the alpha-actinin rod reveals an extensive torsional twist. *Structure* **9**, 597-604.

Yoshimura, S. H., Kim, J. and Takeyasu, K. (2003). On-substrate lysis treatment combined with scanning probe microscopy revealed chromosome structures in eukaryotes and prokaryotes. *J. Electron Microsc. (Tokyo)* **52**, 415-423.

Young, K. G. and Kothary, R. (2005). Spectrin repeat proteins in the nucleus. *BioEssays* **27**, 144-152.

Young, K. G., Pool, M. and Kothary, R. (2003). Bpag1 localization to actin filaments and to the nucleus is regulated by its N-terminus. *J. Cell Sci.* **116**, 4543-4555.

Youssoufian, H., McAfee, M. and Kwiatkowski, D. J. (1990). Cloning and chromosomal localization of the human cytoskeletal alpha-actinin gene reveals linkage to the beta-spectrin gene. *Am. J. Hum. Genet.* **47**, 62-71.

Zhang, Z. Q., Bish, L. T., Holtzer, H. and Sweeney, H. L. (2009). Sarcomeric-alpha-actinin defective in vinculin-binding causes Z-line expansion and nemaline-like body formation in cultured chick myotubes. *Exp. Cell Res.* **315**, 748-759.